Iran. J. Biotechnol. April 2021;19(2): e2623 DOI: 10.30498/IJB.2021.2623

Research Article

Atrazine Promoted Epithelial Ovarian Cancer Cells Proliferation and Metastasis by Inducing Low Dose Reactive Oxygen Species (ROS)

Junyu Chen[1#], Jian Liu[1#], Shan Wu[1], Wei Liu[2], Yang Xia[3], Jing Zhao[1], Yanrong Yang[4], Yuan Wang[5], Yuanqing Peng[1], Shuhua Zhao[1*]

[1] Department of Obstetrics and Gynecology, The Second Hospital of Jilin University, Changchun 130041, China
[2] Research Center of Circular Economy and Pollution Prevention and Control, Jilin Academy of Environmental Sciences, Changchun 130021, China
[3] Department of Pathology, The Second Hospital of Jilin University, Changchun 130021, China
[4] Tongji University, School of Medicine, Shanghai 200092, China
[5] School of nursing, Jilin University, Changchun 130021, China

**Corresponding author:* Shuhua Zhao, Department of Obstetrics and Gynecology, The Second Hospital of Jilin University, Changchun 130041, China; Tel: +86-81136726; E-mail: zhaoshuhua-1966@163.com

 # equal contributors

Background: Atrazine (ATZ) is a triazine herbicide that is widely used in agriculture and has been detected in surface and underground water. Recently, laboratory and epidemiological research have found that the bioaccumulation of ATZ in the environment leads to biotoxicity in the human immune and endocrine systems and results in tumor development.

Objective: To investigate the effects of ATZ exposure on epithelial ovarian cancer (EOC) cells and elucidate the potential mechanisms governing these effects.

Materials and Methods: The human EOC cell lines Skov3 and A2780 were used in this study to explore the effects and mechanisms of ATZ exposure on EOC. The mouse embryonic osteoblastic precursor MC3T3-E1 cells served as the control cells to determine the effects of ATZ on cancer cell lines. After exposure to ATZ, the MTT assay, flow cytometry, the colony formation assay, immunohistochemical staining, the cell scratch assay, and the Transwell assay were used to evaluate the proliferative activity, invasion, and migration capabilities of EOC cell lines. Moreover, flow cytometry was also applied to detect the level of reactive oxygen species (ROS) in these two EOC cell lines, as well as the MC3T3-E1 cells. To further illustrate the underlying mechanisms governing the effect of ATZ on EOC, real-time PCR and Western blotting were employed to assess the transcription and the expression level of Stat3 signaling pathway-related genes in Skov3 and MC3T3-E1 cells.

Results: The results showed that following ATZ treatment, the cell proliferation, migration, and invasion potencies of Skov3 and A2780 cells were increased compared to those of the control group. Meanwhile, the ROS levels of EOC and MC3T3-E1 cells were notably elevated after ATZ treatment. In Skov3 cells, the expression levels of p53 and p21 were downregulated, while those of Cyclin E, vascular endothelial growth factor (VEGF), matrix metallopeptidase 2 (MMP2), MMP9, signal transducers and activators of transcription 3 (Stat3), and p-Stat3 were upregulated by ATZ treatment. In MC3T3-E1 cells, however, ATZ treatment did not affect the level of p53/p21 mRNA compared to the control groups. Moreover, there was no significant change in the expression levels of Stat3 and p-Stat3 in MC3T3-E1 cells exposed to ATZ. This phenomenon was observed while the proliferation rate was enhanced in MC3T3-E1 cells by ATZ.

Conclusions: The results of this study suggest that ATZ effectively promotes the proliferation and metastasis of EOC cells through the Stat3 signaling pathway by inducing low levels of ROS. Additionally, although ATZ might also induce proliferative potential in normal cells, the mechanisms governing its effects in these cells might be different from those in EOC cells.

Keywords: Atrazine; Epithelial ovarian cancer; Reactive oxygen species (ROS); Stat3

1. Background

Atrazine (ATZ), an herbicide of the triazine class, has been widely used worldwide to increase the production of crops, such as sugarcane, sorghum, and corn, due to its convenience, low cost, and excellent broadleaf weed control efficacy (1). The annual use of ATZ in China is 1000-1500 tons, which accounts for approximately 15% of the global total (70,000-90,000 tons per year) (2, 3). Because ATZ has a stable structure and is difficult to degrade, it has a long residence time in the environment (1). The abuse of ATZ would contribute to the pollution of soil and surface and underground water, which poses a further threat to human health (4). The United States Environmental Protection Agency (US EPA) has set the maximum allowed amount of ATZ in public water supplies and drinking water at 3 $\mu g.L^{-1}$ (5). However, the amount of ATZ in the environment is still notably high due to its overuse. In the midwestern United States, researchers found that the concentration of ATZ in farmland was over 300 $\mu g.L^{-1}$ after rainfall (6). A monitoring study on the soil and groundwater in Qian'an and Gongzhuling of China observed that the detection rates of ATZ in soil and groundwater were 97% and 89%, respectively (7). Some researchers have shown that human exposure to ATZ may be associated with chronic noncancer effects, including long-term immunotoxic effects (8, 9), endocrine disruption (4), and vascular lesions (10), and carcinogenic effects, such as lung, breast, pancreatic, prostate, and ovarian cancers, as well as leukemia (11). Although mechanisms related to the development of carcinomas caused by ATZ exposure have not been fully elucidated, it is suspected that the pathways may include oxidative stress, DNA damage, and chromosome aberration (12). However, the complicated association between ATZ and its carcinogenic risk warrants further investigation. Epithelial ovarian cancer (EOC) is the most lethal gynecological cancer with a five-year survival rate of only approximately 46% (13). Worldwide, 230,000 women are diagnosed with EOC annually, causing 150,000 deaths (14). Many risk factors, such as lifestyle, exogenous hormone use, and reproductive history, have been considered to be the potential etiology of EOC in epidemiological studies (15). Environmental factors have also been investigated, but to date, they have not been conclusively associated with the development of this neoplasm. Albanito found that ATZ could promote EOC cell proliferation (16). Meanwhile, studies have found that the effects of ATZ exposure on EOC are related to various signaling pathways. Albanito revealed that ATZ could regulate the estrogen receptor α pathway in EOC cells and cancer-associated fibroblasts, thereby inducing the proliferation of tumor cells (16). Besides, it was found that ATZ could induce DNA damage and tumorigenesis in frogs (17). Although numerous accounts of laboratory research have provided evidence linking ATZ to a higher risk of EOC, epidemiological research has not identified the link between ATZ and EOC to date (18). Therefore, the specific association between ATZ and increased risk of human EOC needs to be further explored and discussed.

2. Objectives

In this study, to elucidate the effect of ATZ exposure on EOC cells, the human EOC cell lines Skov3 and A2780 were exposed to ATZ, and their proliferation, cell cycle, and metastasis were observed. Meanwhile, the mouse embryonic osteoblastic precursor cell line MC3T3-E1 was also exposed to ATZ to observe the effect of ATZ on normal cells. Moreover, the transcription and expression levels of associated genes were detected. From these results, we precisely identified whether ATZ could increase the proliferation and metastasis ability of human EOC cells *in vitro*. Furthermore, by observing the changes in ROS in Skov3 and A2780 cells, the possible mechanisms governing the carcinogenic effects of ATZ were discussed.

3. Materials and Methods

3.1. Cell Culture

ATZ (99% purity) was obtained from Sigma Chemical Company (St Louis, Missouri, USA). The human EOC cell lines Skov3 and A2780 and the mouse embryonic osteoblastic precursor cell line MC3T3-E1 were obtained from the Basic Medical College of Jilin University.

Skov3, A2780, and MC3T3-E1 cells were cultured in Iscove's Modified Dulbecco's Medium (IMDM, HyClone) supplemented with 10% fetal bovine serum (FBS, Gibco) and incubated at a constant temperature of 37 °C in a 5% CO_2 humidified atmosphere. In the experiments, the EOC cells and MC3T3-E1 cells were exposed to 0.1 μM and 1 μM ATZ in the experimental groups.

3.2. MTT Assay

The proliferation effect of ATZ on Skov3, A2780, and MC3T3-E1 cells was detected by MTT (Sigma-Aldrich, St Louis, MO, USA) reagent *in vitro*, as previously described (19). Briefly, Skov3, A2780, and MC3T3-E1 cells were seeded onto 96-well plates at a density of

3000 cells/well. After incubation for 24 hours, these cells were exposed to ATZ at 0 μM, 0.1 μM, or 1 μM for 24 hours, 48 hours, 72 hours, and 96 hours. Then, an MTT solution (10 μL per well, 5 $\mu g.mL^{-1}$) was added to each well. After being cultured at 37 °C for 4 hours, DMSO solution was added at 150 $\mu L.well^{-1}$to dissolve the precipitate. The absorbance of each well was measured at 490 nm using a Microplate Reader (Biotek, Citation 5, USA). All experiments were represented by three replicates.

3.3. Colony Formation Assay

Skov3 and A2780 cells were seeded onto 6-well plates at a density of 100 cells/well. Two weeks later, the formation of a typical clone of the cells was observed. The cells were fixed with methanol and stained with 10% Giemsa (Biotopped, China). The number of visible colonies was counted to evaluate the colony formation ability of cells. All experiments were represented by three replicates.

3.4. Cell Cycle Detection

Skov3, A2780, and MC3T3-E1 cells were plated in 12-well plates (5×10^4 cells/well) and incubated with different concentrations (0 μM, 0.1 μM, and 1 μM) of ATZ for 48 hours. The cells were stained with 200 μL (50 $\mu g.mL^{-1}$) of propidium iodide (PI) solution according to the manufacturer's instructions (Biotopped, China). The flow cytometer (BD FACSCalibur, USA) was used for single parameter analysis, and the cumulative curve segmentation method was used to calculate the percentage of cells in each phase. All experiments were represented by three replicates.

3.5. Cell Scratch and Transwell Assay

For the cell scratch assay, Skov3 and A2780 cells were seeded onto 6-well plates (6×10^5 cells/well). After being cultured at 37 °C for 24 hours, the cells were divided in to 3 groups: the control group (ATZ 0 μM), the low-dose group (ATZ 0.1 μM) and the high-dose group (ATZ 1 μM). The cellular layer was scratched using a plastic pipette tip after 80% of the cells had merged. The migration rate of the cells at the edge of the scratch was analyzed after 48 hours. All experiments were represented by three replicates.

For the invasion assay, following 12 hours of serum-starvation treatment, Skov3 and A2780 cells were adjusted to a concentration of 3×10^4 cells/mL using serum-free media (containing or not containing ATZ), respectively. Then, 100 μL single-cell suspension was added to the apical chamber (8 μm polycarbonate membrane, Corning) coated with collagen, and 600 μL IMDM with 10% FBS (containing or not containing ATZ) was added to the bottom chamber. The cells were allowed to invade through the collagen-coated polycarbonate membrane for 40 hours at 5% CO_2 and 37 °C. Then, the cells remaining on the upper surface were wiped off with a cotton ball. The cells that had invaded were fixed and stained with 10% Giemsa. The cells were then observed and counted in 5 random fields of view (400×) (20). All experiments were represented by three replicates.

3.6. ROS Detection

ROS generation was determined by flow cytometry analysis using the fluorescent chemiluminescent probe 2',7'-dichlorofluorescein (H2DCFDA) (Biyuntian, Shanghai, China). Briefly, Skov3, A2780, and MC3T3-E1 cells were grown in 6-well plates at 1×10^5 cells/well and treated with different concentrations of ATZ for 48 hours. After that step, the treated cells were collected by centrifugation and incubated with H2DCFDA (10 μM) for 30 minutes at 37 °C. Then, the cells were washed with PBS three times and cultivated with serum-free medium for 10 minutes at 37 °C. Finally, the mean fluorescence intensity of ROS in each group was measured using flow cytometry.

3.7. Real-time PCR

Skov3 and MC3T3-E1 cells were seeded at a density of 6×10^5 cells per well and were treated with ATZ for 48 hours. Total RNA was extracted using TRIzol reagent (Invitrogen Company, USA), and first-strand cDNA synthesis was performed using a cDNA synthesis kit (TaKaRa, China). Real-time PCR was used to detect the transcription of p21 and p53 by the SYBR Green real-time PCR kit (TaKaRa, China), and GAPDH was used as an internal control gene. The gene primers for Skov3 cells in PCR are shown in **Table 1**. The gene primers for MC3T3-E1 cells in PCR were supplied

Table 1. Primers for p21, p53 and GAPDH

Gene	Primers (5'→3')
P21	ACCTTCGACTTTGTCACCGAGA
	GCAGGCACAAGGGTACAAGACA
P53	GGCCATCTACAAGCAGTCACAG
	AGCAAATCTACAAGCAGTCACAG
GAPDH	GGAAAGGCTGGGGCTCATTTG
	AGAAGGGGCCATCCACAGTCTTC

by the Genecopoeia company (Guangzhou, China): p53 (MQP030403), p21 (MQP072719), and GAPDH (MQP027158). PCR was performed at 94 °C for 30 seconds followed by 45 cycles of amplification at 94 °C for 5 seconds, 51 °C for 15 seconds, and 72 °C for 10 seconds by using ABI-Q3 (Thermo Fisher, China). The results were repeated at least three times independently.

3.8. Western Blot Analysis

Soluble proteins were extracted from three groups of cells and separated through 12% SDS-polyacrylamide gels. Prestained standards (Invitrogen, USA) were used as molecular weight markers. Separated proteins were transferred to polyvinylidene difluoride (PVDF) membranes (iBlot system, Invitrogen). The membranes were then blocked with 5% skim milk and incubated at room temperature with primary antibodies for 4 hours, including rabbit anti-Stat3 (1:1500, AF6294), rabbit anti-p-Stat3 (1:1500, AF3293), rabbit anti-VEGF (1:1500, AF5131), rabbit anti-MMP2 (1:1500, AF5330), rabbit anti-MMP9 (1:1500, AF5228), rabbit anti-CyclinE (1:1500, AF0144), rabbit anti-p21 (1:1500, AF6290), rabbit anti-p53 (1:1500, AF0879) and rabbit anti-β-actin (1:1500, AF7018). These primary antibodies were all purchased from Affinity Company (China). After incubation with secondary HRP antibodies (1:4000, Bioss, China, bs-0295G-HRP) for 1 hour at room temperature, the protein levels were detected with an ECL plus kit (Millipore, USA), and the densities of the specific bands were quantified with an imaging densitometer (Clinx Science Instruments Company, China). The results were repeated at least three times independently.

3.9. Immunohistochemical (IHC) Staining

The coverslips were placed in the bottom of 24-well plates. After adjusting to 2×10^5 cells.mL^{-1}, 1 mL single Skov3 cell suspension was added to each well of the plates and then incubated for 24 hours at 5% CO_2 and 37 °C. Subsequently, the cells were treated with different concentrations of ATZ for 48 hours, which was prepared for proliferating cell nuclear antigen (PCNA) IHC staining. For IHC staining, standard IHC procedures were carried out as previously described (21). Rabbit anti-human PCNA (1:300, Bioss, bs-0754R) was used as the primary antibody, and biotinylated goat anti-rabbit IgG (1:500, Bioss, bs-0295G-Bio) was used as the secondary antibody. The slices were evaluated by Image-Pro Plus 6.0, and positive cells were identified as cells with brown staining. The results were repeated at least three times independently.

3.10. Statistical Analysis

All experiments were represented by three replicates. SPSS 17.0 (SPSS Inc, Chicago, IL, USA) was employed for statistical analysis. Data are presented as the mean±s.d. Statistical analysis was performed for multiple comparisons using a one-factor analysis of variance (ANOVA). $P<0.05$ was considered to be significant, and $P<0.01$ was considered to be significant.

4. Result

4.1. ATZ Could Promote the Proliferation of EOC and MC3T3-E1 Cells

The MTT assay results showed that EOC cells treated with 1 μM ATZ for 48 hours, 72 hours or 96 hours exhibited a significant increase in cell proliferation rates compared to the cells treated with ATZ-free conditions. Moreover, the rates of the low-dose groups were also significantly higher than those of the control groups (**Fig. 1, A and B**). Interestingly, the noncancer MC3T3-E1 cells also presented an obvious increase in cell proliferation rates after being treated with ATZ for 24 hours, 48 hours, and 72 hours, regardless of the dose of ATZ. However, there was a decreasing tendency in the cell proliferation rates of MC3T3-E1 cells (**Fig. 1C**). Furthermore, after being treated with both low-dose and high-dose ATZ, the colony ability of EOC cells was significantly enhanced compared to that of the control group (**Fig. 1D, E, F, and D**). Moreover, compared with the control group, the Skov3 cell number and positive rates of PCNA expression were dose-dependently higher after treatment with 0.1 μM and 1 μM ATZ (**Fig. 4A**). The results indicated that the proliferation of EOC and MC3T3-E1 cells exposed to ATZ was accelerated.

4.2. ATZ Could Accelerate EOC and MC3T3-E1 Cell Cycle Progression

The results of PI staining in flow cytometry showed an increase in EOC cell numbers in the S phase and a decrease in G0/G1 phase both in the 0.1 μM and 1 μM groups compared to the control group (**Fig. 1 H, I, J and K**). Moreover, ATZ also increased the proportion of cells in the G2/M phase while decreasing the ratio of cells in G1/G0 phase in MC3T3-E1 cells (L, M). These results indicated that ATZ promoted EOC and MC3T3-E1 cell proliferation by accelerating cell cycle progression.

4.3. ATZ Could Promote EOC Cell Invasion and Migration

As shown in the cell scratch assay, the migration rates

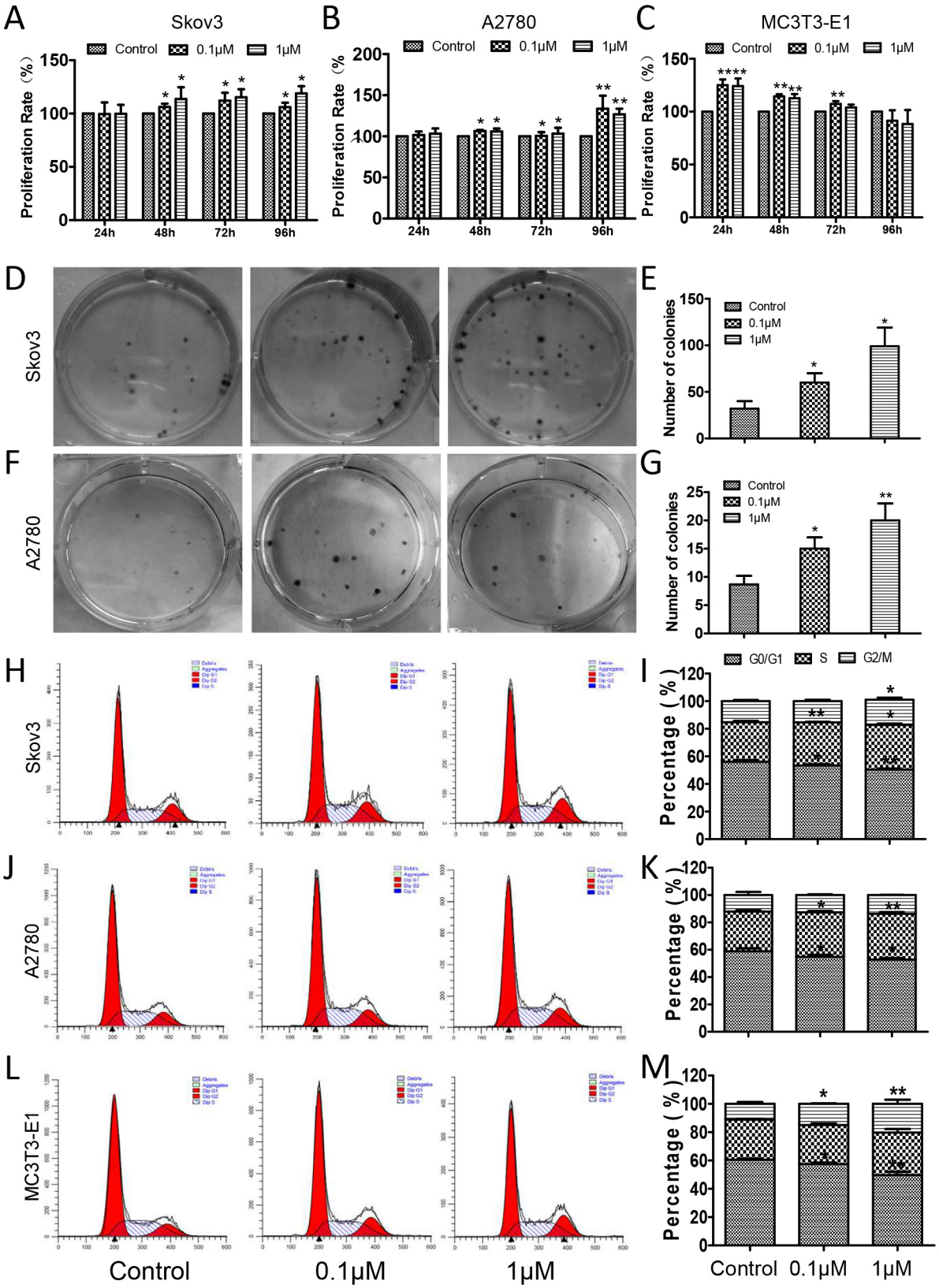

Figure 1. ATZ exposure promoted the proliferation of Skov3, A2780, and MC3T3-E1 cells. MTT assays were performed to examine the proliferation rates of (A) Skov3, (B) A2780, and (C) MC3T3-E1 cells. Colony formation assays were employed to assess the proliferation ability of (D, E) Skov3 and (F, G) A2780 cells. Flow cytometry analysis was carried out to test the cycle progression of (H, I) Skov3, (J, K) A2780, and (L, M) MC3T3-E1 cells. *, $p<0.05$ vs control group, * *, $p<0.01$ vs control group

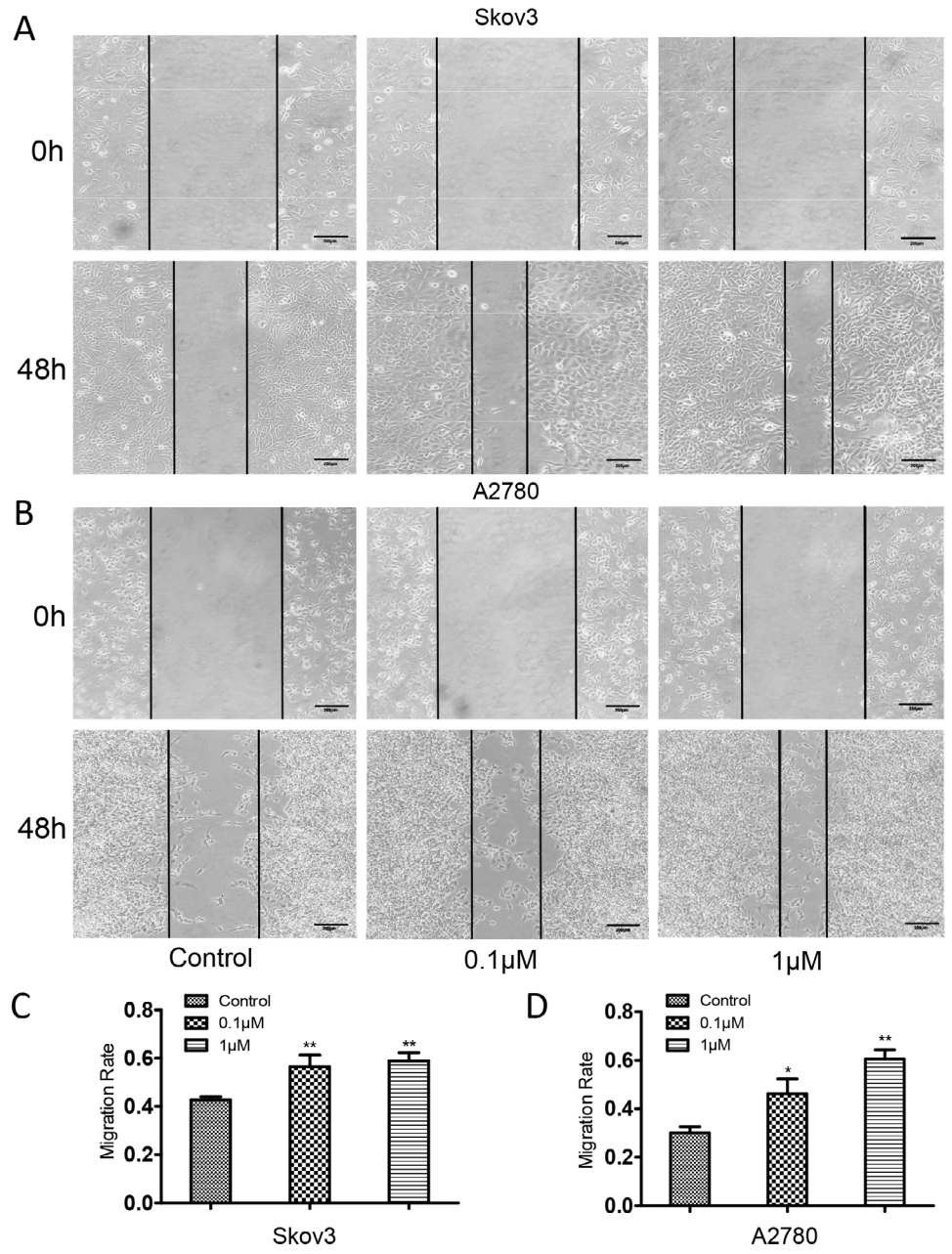

Figure 2. ATZ enhanced the migration ability of EOC cells. A cell scratch assay was used to observe the migration ability of (A, C) Skov3 and (B, D) A2780 cells. *, $p<0.05$ vs control group, * *, $p<0.01$ vs control group.

of ATZ-treated cells (0.1 μM or 1 μM) at the scratch edge were significantly increased compared to the control group (**Fig. 2**). The experiment confirmed that cells exposed to ATZ had a stronger migration ability than cells with ATZ-free. Furthermore, a Transwell assay was used to detect the invasion ability of EOC cells treated with ATZ. After exposure to ATZ, the number of cells invading through the polycarbonate membrane significantly increased in the ATZ exposure groups (**Fig. 3 A, B, C, and D**), indicating that ATZ could enhance the invasion ability of EOC cells. Hence, the experimental data above confirmed that ATZ could enhance EOC cell invasion and migration, implying the notable role of ATZ in the metastasis of EOC cells.

4.4. ATZ Exposure Could Increase Intracellular ROS Level

Low levels of ROS might be a key driver of tumor initiation and development. The ROS level was increased dose-dependently in the ATZ groups

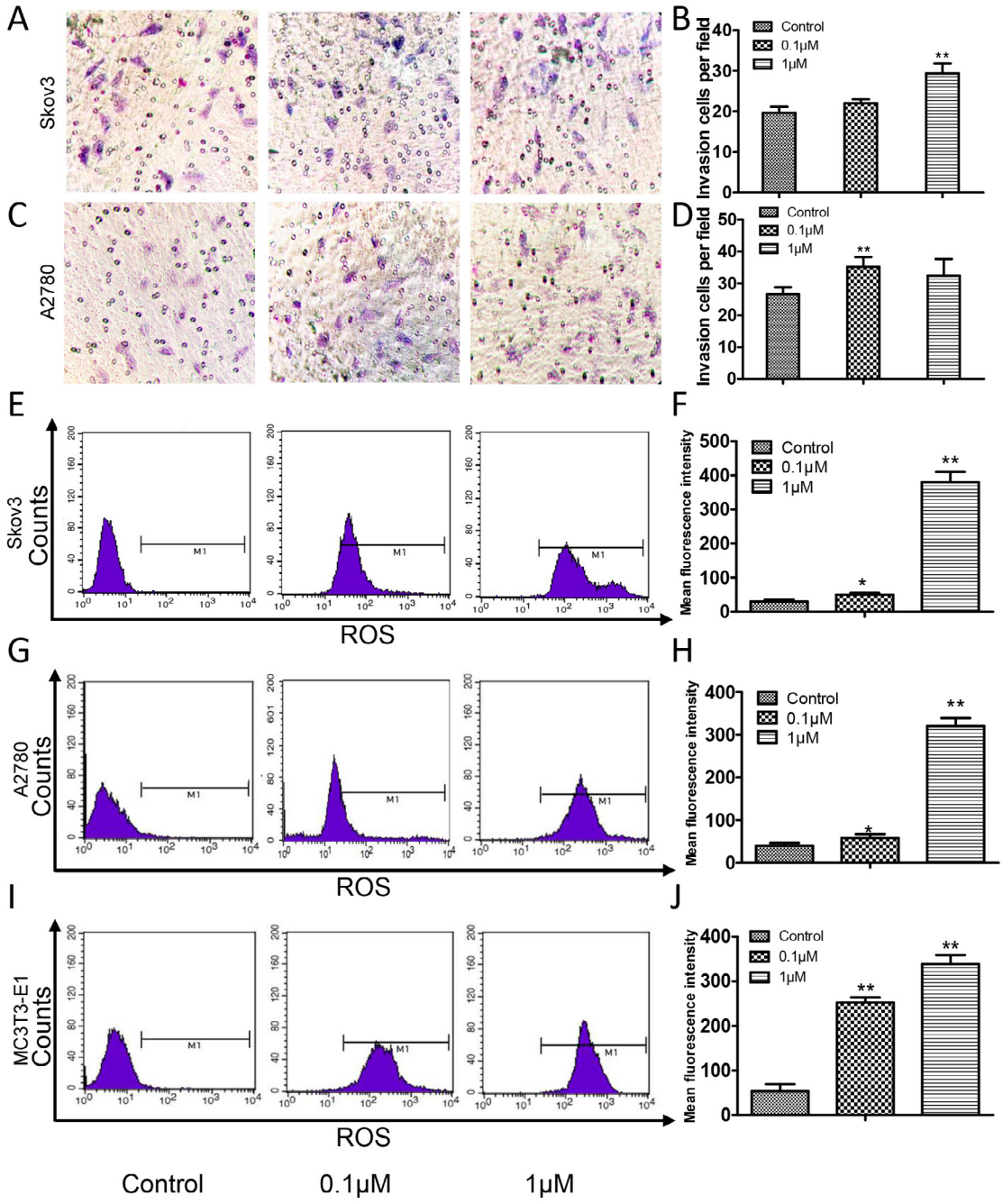

Figure 3. ATZ strengthened the invasion ability of EOC cells and increased intracellular ROS levels. A Transwell assay was conducted to assess the invasion capacity of (A, B) Skov3 and (C, D) A2780 cells. Flow cytometry was applied to analyze the level of ROS in (E, F) Skov3, (G, H) A2780, and (I, J) MC3T3-E1 cells. *, p<0.05 vs control group, * *, p<0.01 vs control group

compared to the control group, implying that ATZ may promote EOC cell proliferation and metastasis *in vitro* by producing low levels of ROS (**Fig. 3 E, F, G, and H**). Interestingly, we found that low levels of ROS were also generated by ATZ in MC3T3-E1 cells (**Fig. 3 I and J**), suggesting that ATZ might accelerate the proliferation of noncancerous cells by inducing ROS in a short time.

4.5. ATZ Downregulates p53 and p21 while upregulates Cyclin D1 in Skov3 Cells

As shown in **Figure 4 B and C**, the transcriptional levels of p53 and p21 were significantly downregulated in Skov3 cells after ATZ exposure compared to those of the control group. However, we did not find any significant changes in the level of p53 or p21 mRNA in MC3T3-E1 cells treated with ATZ (**Fig. 5 A and**

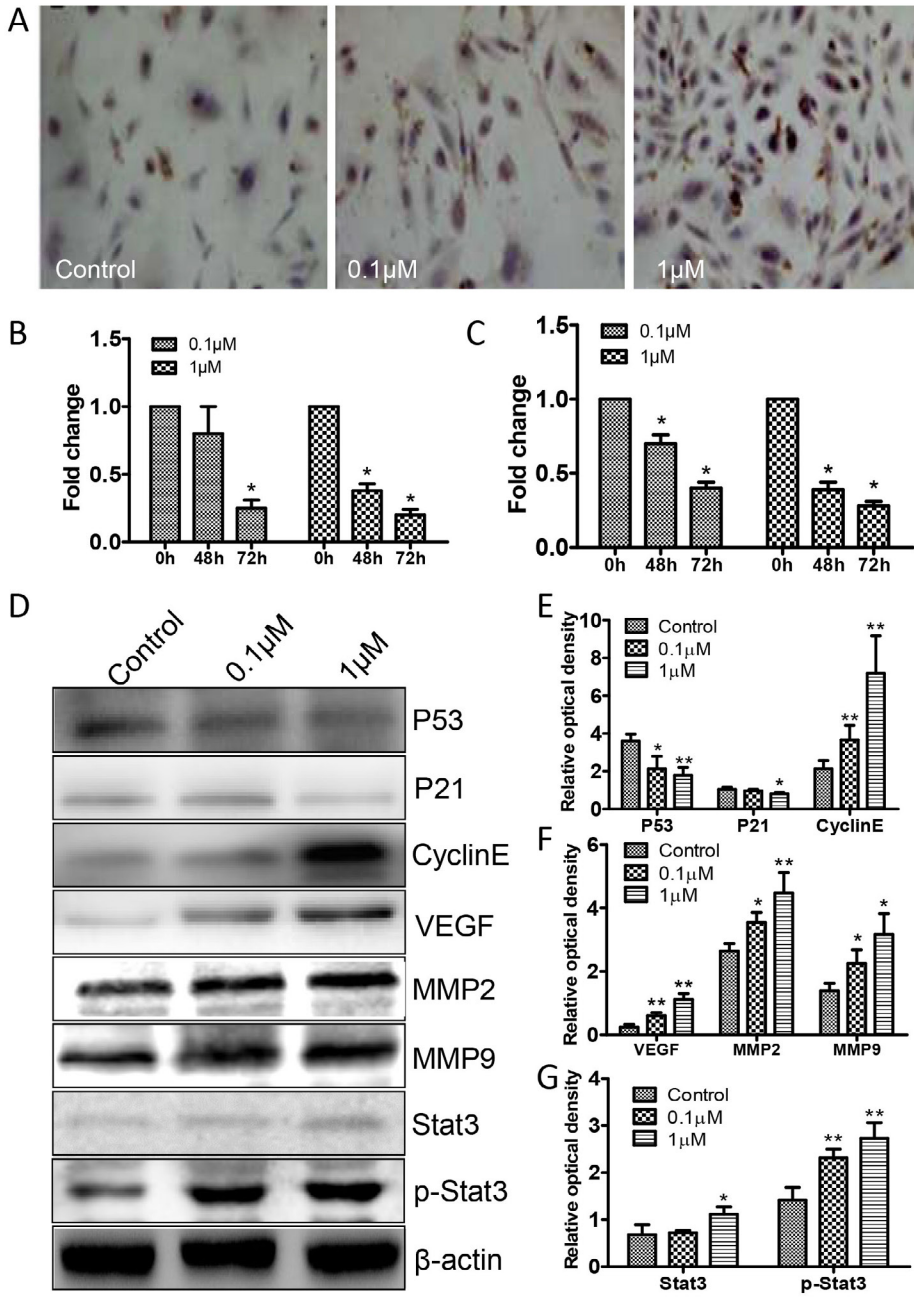

Figure 4. ATZ accelerated the proliferation and metastasis of Skov3 cells by activating the Stat3 signaling pathway. (A) IHC staining was carried out to delineate the expression of PCNA protein in Skov3 cells. Real-time PCR was employed to detect the transcriptional levels of (B) P53 and (C) P21. (C, D, E, and F) Western blot analysis was conducted to measure key proteins of several signaling pathways. *, $p<0.05$ vs control group, * *, $p<0.01$ vs control group

B). After that step, Western blotting was used to detect the expression of p53, p21, and Cyclin E. The results showed that ATZ exposure for 48 hours could significantly downregulate the expression of p53 and p21 and upregulate the expression of Cyclin E in Skov3 cells compared to that of the control group (**Fig. 4 D and E**). Taken together, these results indicated that ATZ strongly promoted cell cycle progression by downregulating the expression of p53 and p21 and upregulating the expression of Cyclin E.

4.6. ATZ Could Upregulate MMP2, MMP9, and VEGF Expressions in Skov3 Cells

To further investigate the mechanism of ATZ-induced metastasis in Skov3 cells, Western blot analysis was employed to detect the metastasis-associated proteins

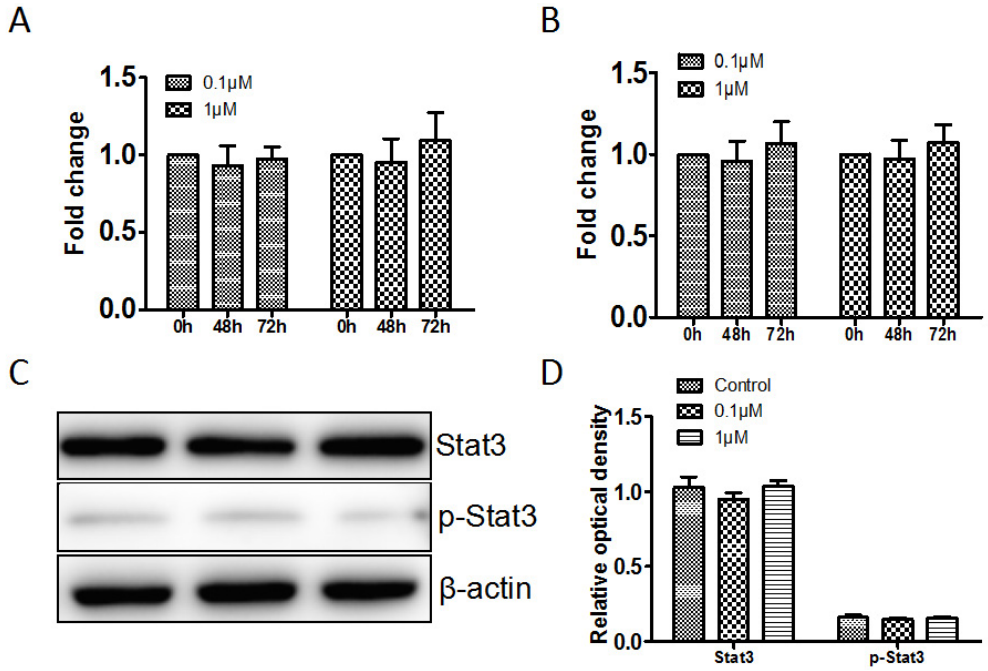

Figure 5. ATZ impacted the proliferation and cell cycle in MC3T3-E1 cells, possibly not by regulating the transcription of P53/P21 and the expression of Stat3/p-Stat3. Real-time PCR was used to detect the transcriptional levels of (A) P53 and (B) P21. Western blotting was applied to evaluate the expression of Stat3 and p-Stat3. *, $p<0.05$ vs control group, * *, $p<0.01$ vs control group

MMP2, MMP9, and VEGF. The expression of MMP2, MMP9, and VEGF in the ATZ treatment group was significantly upregulated in a dose-dependent manner compared with the control group. These results indicated that ATZ might promote EOC metastasis by upregulating MMP2, MMP9, and VEGF (**Fig. 4 D and F**).

4.7. ATZ Could Promote the Activation of Stat3 in Skov3 Cells

Stat3 is essential for cell survival and proliferation. In our study, the expression of Stat3 and p-Stat3 was significantly upregulated in the ATZ exposure groups compared to the control group, which indicated that ATZ could promote the proliferation and metastasis of Skov3 through the Stat3 signaling pathway (**Fig. 4 D and G**). However, ATZ did not increase the expression of Stat3/p-Stat3 proteins in MC3T3-E1 cells (**Fig. 5 C and D**).

5. Discussion

Epidemiological studies have shown that atrazine (ATZ) has a higher risk of damage to the endocrine and reproductive systems, as well as numerous other organs, which may lead to chronic noncancerous or cancerous diseases (4, 9-11, 22). Epithelial ovarian cancer (EOC) is the seventh most commonly diagnosed form of cancer among women worldwide. Epidemiologists have further reported that environmental contamination may be a driving factor for EOC (13, 15). However, the direct correlative environmental factors causing EOC have not been determined to date. In recent studies, EOC cells were used to further identify the mechanism of ATZ and its degree of impact on the growth and metastasis of human EOC cells. Additionally, MC3T3-E1 cells, which are normal noncancerous cells, were compared to EOC cells.

In MTT and colony formation assays, we found that ATZ exposure promoted the proliferation of EOC cells in a dose- and time-dependent manner, which was in keeping with findings obtained with BG-1 and OV2008 cells in a previous study(16). Although the results of the MTT assay initially showed that ATZ significantly enhanced the proliferation ability of MC3T3-E1 cells, the effects progressively diminished after 48 hours and 72 hours, respectively. The enhancement effect on MC3T3-E1 cells disappeared after 96 hours of ATZ treatment. PCNA, a regulator of cell growth function, is a well-known molecular marker for cell proliferation. High-level expression of PNCA indicates the vigorous proliferation ability of cells(23). Subsequent immunohistochemical staining also showed that the expression of PCNA was upregulated in the nucleus of Skov3 cells after exposure to ATZ. These results implied both that the proliferation ability of EOC cells could be enhanced by ATZ in a time-dependent way and that

normal noncancerous cells could also produce a similar reaction over a short period. Nevertheless, the cytotoxic effect of ATZ on normal cells might be gradually strengthened over a long period and ultimately harm organ systems. Instead, neither low-dose nor high-dose ATZ exhibited a clear cytotoxic effect on EOC cells.

To further investigate the mechanism by which ATZ enhanced the proliferation ability of EOC and MC3T3-E1 cells, the cell cycle distribution was examined after ATZ exposure. We found that ATZ promoted EOC cells to pass through the G1/S phase checkpoint, decreased the cell numbers in G0/G1 phase, and finally caused the accumulation of Skov3 cells in the S phase. S phase is reported to contribute to DNA synthesis, replication, and repair, suggesting that ATZ might promote cell growth by S phase arrest(24). To demonstrate the molecular mechanism by which ATZ impacts the cell cycle, the mRNA and protein levels of genes associated with the cell cycle were monitored. The cell cycle regulatory pattern is regulated by multiple checkpoints at different phases. Among these checkpoints, G1/S is an important checkpoint. p53 and p21 play key roles in G1/S arrest. Specifically, p53 induces the transcription of the cell cycle-related gene p21, and p21 binds to the CDK2/CyclinE complex and finally causes G1/S arrest(25, 26). Our results showed that ATZ exposure downregulated the transcription and expression of p53 and p21 while increasing the expression of CyclinE, which might accelerate the transition from G0/G1 to the S phase and lead to S phase arrest. Accordingly, the hypothesis is that ATZ can improve both DNA synthesis and damaged DNA repair by inducing S arrest, which would further suggest that ATZ could induce EOC cells to pass through the G1/S checkpoint, blocking them in the S phase. Furthermore, our study showed a decrease in the G0/G1 phase proportion and an increase in the G2/M phase proportion in MC3T3-E1 cells treated with ATZ, which might suggest that the proliferative potential of MC3T3-E1 cells was activated by ATZ. However, ATZ did not decrease the level of p53/p21 mRNA in MC3T3-E1 cells, which meant that ATZ accelerated the cell cycle of MC3T3-E1 cells by other mechanisms, which warrants further research to explore.

Invasion and migration are two major processes of tumor cell metastasis. Transwell and cell scratch assays verified that ATZ promoted the invasion and migration of EOC cells. To clarify the underlying molecular mechanism of this ability, a series of related proteins, including MMP2, MMP9, and VEGF, were detected in our study. It has been reported that matrix metalloproteinases (MMPs), such as MMP2 and MMP9, can dissolve small holes that allow cancerous cells to invade into the stromal membrane surrounding blood vessels (27). The results showed that the expression of MMP2 and MMP9 in Skov3 cells was significantly increased after exposure to ATZ, which indicated that ATZ exposure enhanced the invasion ability of EOC cells by upregulating MMP2 and MMP9 expression. VEGF plays an important role in the formation of blood vessels in physiological and pathological cancer progression. Additionally, VEGF is essential for tumor cell migration(23). In this study, the expression of MMP2, MMP9, and VEGF in Skov3 cells was significantly upregulated after ATZ exposure, which suggested that ATZ could promote metastasis in EOC cells.

Signal transducers and activators of transcription 3 (Stat3), an oncogene, contribute to inducing cancer cell survival, proliferation, and metastasis in numerous cancers, including EOC (28-30). Using Skov3 cells, we found that ATZ upregulated the expression of Stat3, thereby enhancing its activity. Consequently, the inductive effect of ATZ on Stat3 activation resulted in vigorous cell proliferation and malignant metastasis. Moreover, ATZ exposure upregulated MMP2, MMP9, VEGF, and CyclinE while downregulating the expression of p53 and p21. Therefore, ATZ promoted EOC proliferation and metastasis by mediating the activation of the Stat3 signaling pathways. Furthermore, we investigated the potential mechanism by which ATZ activated the Stat3 pathway. Our study showed that ATZ could induce the production of intracellular reactive oxygen species (ROS). ROS are a series of chemical compounds containing oxygen produced during cellular metabolism, including superoxide anion (O^{2-}), hydroxyl radical (OH^{-}), and hydrogen peroxide (H_2O_2), and these chemicals could have a negative effect on lipids, proteins, and DNA(31). Reports have suggested that low levels of ROS could initiate carcinogenesis and help tumor cells survive and metastasize (32). Interestingly, it has been reported that Stat3 is directly sensitive to ROS(33). These results imply that ROS may play an important role in promoting the proliferation and metastasis capacity of EOC cells by activating the Stat3 signaling pathway after ATZ exposure. Although the expression of Stat3/p-Stat3 was not changed in MC3T3-E1 cells treated with ATZ, we found that low levels of ROS were produced in the cells, which might be the reason for its cell proliferation and cell cycle changes. The reason for the difference in Stat3/p-Stat3 expression between normal and cancerous cells might be related to its different activation extents. As an oncogene, Stat3 is generally active in many tumor

cells and easily upregulated by some carcinogenic factors, such as ROS (33). In normal cells, however, Stat3 might be in a non-active state, which could not be activated or upregulated by such low-level ROS caused by ATZ in a short period. Thus, we hypothesized that the proliferation of MC3T3-E1 cells was enhanced by low levels of ROS caused by ATZ via other cell signaling pathways instead of the Stat3 pathway. Collectively, ROS caused by ATZ might have specific mechanisms of pro-proliferation on normal cells, which is different from the mechanisms governing the effect of ATZ on cancer cells. However, whether the effect of ROS caused by ATZ is a threat and the mechanisms of its pro-proliferation effect on normal cells merit further exploration.

6. Conclusions

We demonstrated that ATZ promoted the proliferation and metastasis of EOC cells, as well as the proliferation of MC3T3-E1 cells. Based on the effective promotion of cell proliferation and metastasis by ATZ, we proposed a possible mechanism by which ATZ activates the Stat3 signaling pathway by inducing the production of low-level ROS, which consequently results in the activation of a variety of signal molecules in EOC cells. These activated signal molecules subsequently promote the malignant progression of EOC cells, thereby driving increased proliferation and metastasis.

Acknowledgments

This study was supported by the project of the Jilin Province Development and Reform Commission (2014G073), the project of the Jilin Province Department of Finance (2019SCZT050), and the project of the Jilin Province Department of Finance (2019SCZT040).

References

1. He H, Liu Y, You S, Liu J, Xiao H, Tu Z. A Review on Recent Treatment Technology for Herbicide Atrazine in Contaminated Environment. *Int J Environ Res Public Health*. 2019;**16**(24):5219. https://doi.org/10.3390/ijerph16245129
2. Cong, Zhang, Lei, Qin, Da C, Dou, *et al*. Atrazine induced oxidative stress and mitochondrial dysfunction in quail (Coturnix C. coturnix) kidney via modulating Nrf2 signaling pathway. *Chemosphere.* 2018;**212**:974-982. https://doi.org/10.1016/j.chemosphere.2018.08.138
3. Yue L, Ge CJ, Yu H, Deng H, Fu B. Adsorption–desorption behavior of atrazine on agricultural soils in China. *J Environ Sci-china*. 2017;**57**:180-189. https://doi.org/10.1016/j.jes.2016.11.002
4. Mukherjee D, Kar S, Mandal A, Ghosh S, Majumdar S. Immobilization of tannery industrial sludge in ceramic membrane preparation and hydrophobic surface modification for application in atrazine remediation from water. *J Eur Ceram Soc*. 2019;**39**(10):3235-3246. https://doi.org/10.1016/j.jeurceramsoc.2019.04.008
5. Kueseng P, Nisoa M, Sontimuang C. Rapid preparation of molecularly imprinted polymers by custom-made microwave heating for analysis of atrazine in water. *J Sep Sci*. 2018;**41**(13):2783-2789. https://doi.org/10.1002/jssc.201800198
6. Wirbisky-Hershberger SE, Sanchez OF, Horzmann KA, Thanki D, Freeman JL. Atrazine exposure decreases the activity of DNMTs, global DNA methylation levels, and dnmt expression. *Food Chem Toxicol*. 2017;**109**(Pt 1):727-734. https://doi.org/10.1016/j.fct.2017.08.041
7. Geng Y, Ma J, Jia R, Xue Lq, Tao Cj, Li Cj, *et al*. Impact of Long-Term Atrazine Use on Groundwater Safety in Jilin Province, China. *J Integr Agr*. 2013;**12**(2):305-313. https://doi.org/10.1016/s2095-3119(13)60229-4
8. Zhao S, Liu J, Zhao F, Liu W, Li N, Suo Q, *et al*. Sub-acute exposure to the herbicide atrazine suppresses cell immune functions in adolescent mice. *Biosci Trends*. 2013;**7**(4):193-201 .https://doi.org/10.5582/bst.2013.v7.4.193
9. Ida, Holásková, Meenal, Elliott, Kathleen, Brundage, *et al*. Long-term Immunotoxic Effects of Oral Prenatal and Neonatal Atrazine Exposure. *Toxicol Sci.* 2019;**168**(2):497-507. https://doi.org/10.1093/toxsci/kfz005
10. Elisa DOS, Pauliane dMC, Batista dNS, Victor dCW, Maciel dARRI, Batista dSH, *et al*. Atrazine promotes immunomodulation by melanomacrophage centre alterations in spleen and vascular disorders in gills from Oreochromis niloticus. *Aquat Toxicol*. 2018;**202**:57-64. https://doi.org/10.1016/j.aquatox.2018.06.018
11. Brasil VLM, Ramos Pinto MB, Bonan RF, Kowalski LP, da Cruz Perez DE. Pesticides as risk factors for head and neck cancer: a review. *J Oral Pathol Med.* 2018;**47**(7):641-651. https://doi.org/10.1111/jop.12701
12. Mokarizadeh A, Faryabi MR, Rezvanfar MA, Abdollahi M. A comprehensive review of pesticides and the immune dysregulation: mechanisms, evidence and consequences. *Toxicol Mech Method*. 2015;**25**(4) 258-278. https://doi.org/10.3109/15376516.2015.1020182
13. Lheureux S, Gourley C, Vergote I, Oza AM. Epithelial ovarian cancer. *Lancet*. 2019;**393**(10177):1240-1253. https://doi.org/10.1016/s0140-6736(18)32552-2
14. Ferlay J, Soerjomataram I, Dikshit R, Eser S, Mathers C, Rebelo M, *et al*. Cancer incidence and mortality worldwide: sources, methods and major patterns in GLOBOCAN 2012. *Int J Cancer*. 2015;**136**(5):E359-386. https://doi.org/10.1002/ijc.29210
15. Webb PM, Jordan SJ. Epidemiology of epithelial ovarian cancer. *Best Pract Res Clob*. 2017;**41**:3-14. https://doi.org/10.1016/j.bpobgyn.2016.08.006
16. Albanito L, Lappano R, Madeo A, Chimento A, Prossnitz ER, Cappello AR, *et al*. Effects of atrazine on estrogen receptor α- and G protein-coupled receptor 30-mediated signaling and proliferation in cancer cells and cancer-associated fibroblasts. *Environ Health Perspect*. 2015;**123**(5):493-499. https://doi.org/10.1289/ehp.1408586
17. Lim S, Sun YA, Song IC, Chung MH, Jang HC, Park KS, *et al*. Chronic Exposure to the Herbicide, Atrazine, Causes Mitochondrial Dysfunction and Insulin Resistance. *Plos One*. 2009;**4**(4):e5186. https://doi.org/10.1371/journal.pone.0005186
18. Young HA, Mills PK, Riordan DG, Cress RD. Triazine Herbicides and Epithelial Ovarian Cancer Risk in Central

California. *J Occup Environ Med.* 2005;**47**(11):1148-1156. https://doi.org/10.1097/01.jom.0000177044.43959.e8
19. Wu S, Zhao F, Zhao J, Li H, Chen J, Xia Y, *et al*. Dioscin improves postmenopausal osteoporosis through inducing bone formation and inhibiting apoptosis in ovariectomized rats. *Biosci Trends*. 2019;**13**(5):394-401. https://doi.org/10.5582/bst.2019.01186
20. Chen S, Wang J. HAND2-AS1 inhibits invasion and metastasis of cervical cancer cells via microRNA-330-5p-mediated LDOC1. *Cancer Cell Int*. 2019;**19**(1):353. https://doi.org/10.1186/s12935-019-1048-y
21. Zheng J, Shuhua Z, Xiaolin Y, Shuang H, Yan LH. Simultaneous targeting of CD44 and EpCAM with a bispecific aptamer effectively inhibits intraperitoneal ovarian cancer growth. *Theranostics*. 2017;**7**(5):1373-88. https://doi.org/10.7150/thno.17826
22. Zhao S, Liu J, Zhao F, Liu W, Li N, Suo Q, *et al*. Sub-acute exposure to the herbicide atrazine suppresses cell immune functions in adolescent mice. *Biosci Trends*. 2013;**7**(4):193-201. https://doi.org/10.5582/bst.2013.v7.4.193
23. Hu KB, Tian Y, Du YW, Huang LD, Chen JY, Li N, *et al*. Atrazine promotes RM1 prostate cancer cell proliferation by activating STAT3 signaling. *Int J Oncol*. 2016;**48**(5):2166-2174. https://doi.org/10.3892/ijo.2016.3433
24. Bártová E, Suchánková J, Legartová S, Malyšková B, Hornáček M, Skalníková M, *et al*. PCNA is recruited to irradiated chromatin in late S-phase and is most pronounced in G2 phase of the cell cycle. *Protpplasma*. 2017;**254**(5):1-9. https://doi.org/10.1007/s00709-017-1076-1
25. Dotto GP. p21(WAF1/Cip1): more than a break to the cell cycle? *Bioschim Biophys Acta*. 2000;**1471**(1):M43-M56. https://doi.org/10.1016/s0304-419x(00)00019-6
26. Yun HJ, Hyun SK, Park JH, Kim BW, Kwon HJ. Widdrol activates DNA damage checkpoint through the signaling Chk2–p53–Cdc25A–p21–MCM4 pathway in HT29 cells. *Mol Cell Biochem*. 2012;**363**(1-2):281-289. https://doi.org/10.1007/s11010-011-1180-z
27. Fink K, Boratyński J. The role of metalloproteinases in modification of extracellular matrix in invasive tumor growth, metastasis and angiogenesis. *Postep Hig Med Dosw*. 2012;**66**:609-628. https://doi.org/10.5604/17322693.1009705
28. Zhao J, Lin W, Cao Z, Liu L, Zhuang Q, Zhong X, *et al*. Total alkaloids of Rubus aleaefolius Poir. inhibit the STAT3 signaling pathway leading to suppression of proliferation and cell cycle arrest in a mouse model of hepatocellular carcinoma. *Oncol Rep*. 2013;**30**(3):1309-1314. https://doi.org/10.3892/or.2013.2585
29. Zheng B, Geng L, Zeng L, Liu F, Huang Q. AKT2 contributes to increase ovarian cancer cell migration and invasion through the AKT2-PKM2-STAT3/NF-κB axis. *Cell Signal*. 2018;**45**:122-131. https://doi.org/10.1016/j.cellsig.2018.01.021
30. Kong D, Chen J, Sun X, Lin Y, Du Y, Huang D, *et al*. GRIM-19 over-expression represses the proliferation and invasion of orthotopically implanted hepatocarcinoma tumors associated with downregulation of Stat3 signaling. *Biosci Trends*. 2019;**13**(4):342-350. https://doi.org/10.5582/bst.2019.01185
31. Glasauer A, Chandel NS. Ros. *Curr Biol.* 2013;**23**(3):R100-102. https://doi.org/10.1016/j.cub.2012.12.011
32. Bayurova E, Jansons J, Skrastina D, Smirnova O. HIV-1 Reverse Transcriptase Promotes Tumor Growth and Metastasis Formation via ROS-Dependent Upregulation of Twist. *Oxid Med Cell Longev*. 2019;**2019**:6016278. https://doi.org/10.1155/2019/6016278
33. Li L, Cheung SH, Evans EL, Shaw PE. Modulation of Gene Expression and Tumor Cell Growth by Redox Modification of STAT3. *Cancer Res*. 2010;**70**(20):8222-8232. https://doi.org/10.1158/0008-5472.can-10-0894